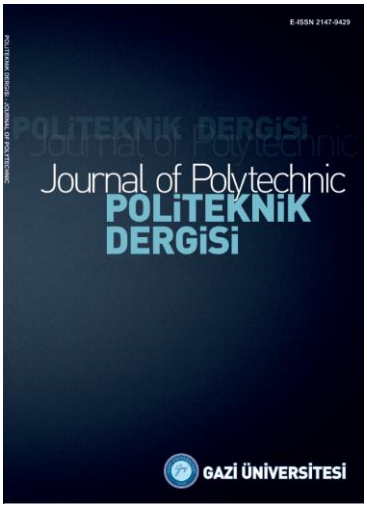

POLİTEKNİK DERGİSİ

JOURNAL of POLYTECHNIC

ISSN: 1302-0900 (PRINT), ISSN: 2147-9429 (ONLINE)
URL: http://dergipark.org.tr/politeknik

Artificial hummingbird algorithm-based PID controller for DC motor speed control

DC motor hız kontrolü için yapay sinek kuşu algoritması tabanlı PID denetleyici

***Yazar(lar) (Author(s))**: Kadir Yasin SUNCA[1], Ali Fuat BOZ[2]*

ORCID[1]: 0009-0006-5024-7820

ORCID[2]: 0000-0001-6575-7678

To cite to this article: Sunca K.Y. ve Boz A.F., "Artificial Hummingbird Algorithm-Based PID Controller for DC Motor Speed Control", ***Journal of Polytechnic***, *(*): *, (*).

Bu makaleye şu şekilde atıfta bulunabilirsiniz: Sunca K.Y. ve Boz A.F., "Artificial Hummingbird Algorithm-Based PID Controller for DC Motor Speed Control", ***Politeknik Dergisi***, *(*): *, (*).

Erişim linki (To link to this article): http://dergipark.org.tr/politeknik/archive

DOI: 10.2339/politeknik.1687239

Artificial Hummingbird Algorithm- Based PID Controller for DC Motor Speed Control

Highlights

- *Artificial Hummingbird Algorithm (AHA)*
- *PID Controllers*
- *DC Motor*
- *Control Parameters*

Graphical Abstract

After modelling the PID-controlled DC motor system, the PID coefficients are optimized using the AHA.

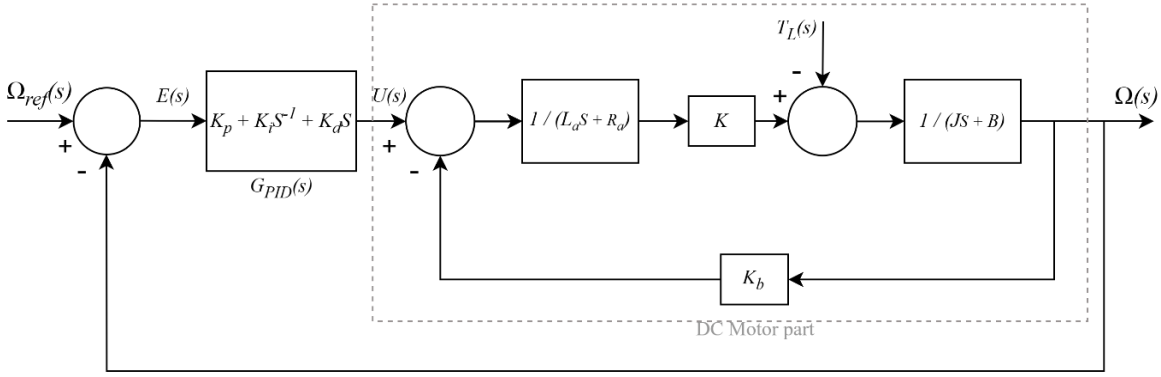

Figure 3. Block schematic of a PID-controlled DC motor system.

Aim

AHA-based PID optimization was used in this study to manage DC motor speed. The outcomes demonstrated that the AHA-PID offered quick and reliable control.

Design & Methodology

In order to manage the speed of a DC motor, a PID controller was created, and the ITAE criterion-based AHA algorithm was used to optimize the parameters.

Originality

This work optimizes PID parameters for regulating the speed of a DC motor using the AHA for the first time, demonstrating improved performance and robustness compared to existing methods.

Findings

Compared to alternative optimization techniques, the AHA-based PID controller produced more stable speed control and quicker rise and settling periods.

Conclusion

When compared to more conventional optimization techniques, the AHA-based PID controller has displayed itself to be trustworthy and efficient remedy for DC motor speed control.

Declaration of Ethical Standards

The researchers involved in this study affirm that neither legal-special nor ethical committee approval is needed for the materials and procedures utilized in this investigation.

Artificial Hummingbird Algorithm- Based PID Controller for DC Motor Speed Control

Araştırma Makalesi / Research Article

Kadir Yasin SUNCA[1*], Ali Fuat BOZ[2]

[1,2] Faculty of Technology, Sakarya University of Applied Sciences, Turkey

(Geliş/Received : 30.04.2025 ; Kabul/Accepted : 03.06.2025 ; Erken Görünüm/Early View : 09.06.2025)

ABSTRACT

The Artificial Hummingbird Algorithm (AHA), a meta-heuristic algorithm that mimics hummingbird feeding behaviours and is a nature-inspired meta-heuristic algorithm proposed by Liying Wang in 2021. This approach uses axial, diagonal, and omnidirectional flight capabilities to carry out migration and foraging processes in a directed manner. The AHA was used in this study to analysed the direct current (DC) motor speed control problem based on proportional-integral-derivative (PID) controllers. The integral of the time-weighted absolute error (ITAE) was employed as an error-based objective function for parameter optimization once the ideal PID parameters (kp, ki, and kd) were identified in the controller design. The AHA was contrasted with other algorithms from the literature at various DC motor operating points in order to increase diversity. The results showed that the results showed that the proposed AHA performed successfully and efficiently for the DC motor speed control problem.

Keywords: AHA, PID Controllers, DC Motor, Control Parameters.

DC Motor Hız Kontrolü için Yapay Sinek Kuşu Algoritması Tabanlı PID Denetleyici

ÖZ

Sinek kuşlarının beslenme davranışlarını taklit eden ve doğadan ilham alan meta-sezgisel bir algoritma olan Yapay Sinek Kuşu Algoritması (AHA), 2021 yılında Liying Wang tarafından yayınlanmıştır. Bu yaklaşım, göç ve yiyecek arama süreçlerini yönlendirilmiş bir şekilde yürütmek için eksenel, çapraz ve çok yönlü uçuş yeteneklerini kullanmaktadır. AHA, bu çalışmada Oransal-İntegral-Türev (OİT) kontrolörlerine dayalı doğru akım (DA) motor hız kontrol problemini analiz etmek için kullanılmıştır. Zaman ağırlıklı mutlak hatanın (ITAE) integrali, kontrolör tasarımında ideal OİT parametreleri (kp, ki ve kd) belirlendikten sonra parametre optimizasyonu için hata tabanlı bir amaç fonksiyonu olarak kullanılmıştır. AHA, çeşitliliği artırmak amacıyla çeşitli DA motor çalışma noktalarında literatürdeki diğer algoritmalarla karşılaştırılmıştır. Sonuçlar, önerilen AHA'nın DA motor hız kontrol problemi için başarılı ve etkili bir performans sergilediğini göstermiştir.

Anahtar Kelimeler: AHA, OİT Denetleyiciler, DA Motor, Kontrol Parametreleri.

1. INTRODUCTION

Researchers, scientists, and engineers have had numerous opportunities in recent years to solve various optimization problems thanks to the continuous advancement of optimization methods. Since these algorithms can solve different problems by finding optimal values across various fields, overcoming local minima remains a critical concern in optimization processes [1]. In this context, the development of optimization techniques has paved the way for innovative solutions in applied engineering fields such as control systems. Particularly in problems requiring precise speed control of DC motors, these algorithms enhance system performance by providing effective and stable responses. The use of DC motors has become an indispensable component of many practical engineering applications to date due to their cost-effectiveness, ease of control, and increased durability [2]. As one of the primary drive components in dynamic systems, DC motors are extensively used in both industrial and academic applications make extensive use of DC motors [3]. One of the most critical parameters that directly affects the performance of these motors is speed control. Especially in applications requiring high precision, effective speed regulation is crucial to ensure system stability and accuracy [4]-[5]. In this sense, in addition to the PID controller, more complex and flexible control systems have lately been extensively examined in the literature. Among these, methods such as fractional-order PID (FOPID) [6], adaptive network-based fuzzy inference system (ANFIS) [7], fuzzy logic-based PID (Fuzzy-PID) [8] and sliding mode control (SMC) [9] stand out, offering effective solutions for improving system performance.

The analysis conducted with the PID controller in this study indicates that, even though it is the most often used method, it is challenging to precisely modify the gain settings [10]. Numerous optimization strategies have been presented in the literature to address this issue and improve the controller's efficacy. In this context, information about optimization techniques used in different studies is presented in Table 1 as a literature summary.

**Sorumlu Yazar (Corresponding Author)*
e-posta : kadirsunca@subu.edu.tr

Table 1. Studies on the DC motor speed control problem in the literature**.**

Ref.	Improved Algorithm	Results
[11]	LFDNM	A new hybrid optimization method for PID controller was developed by combining LFD and Nelder–Mead algorithms. The system optimized according to the ITAE criterion provided better transient response, shorter settling time, and higher stability compared to classical and other meta-heuristic methods.
[12]	mJS	The mJS algorithm, which was improved with Weibull distribution and opposition-based learning for DC motor speed control, was used in this study to optimize PID parameters. In comparison to GWO, JAYA, and GJO, mJS reduced the ITAE value, accomplished a faster settling time, and improved accuracy.
[13]	CSA	The Crow Search Algorithm was used to enhance the PID controller's performance in DC motor speed control. PID parameters were optimized according to different error criteria (ISE, IAE, ITAE). CSA provided more accurate and stable results compared to manual tuning.
[14]	HGSO	The Matsuda method and the HGSO algorithm were used to design a fractional PID (FPID) controller. In comparison to other algorithms, the FPID optimized using the ITAE criterion showed excellent disturbance rejection, reduced overshoot, and a faster settling time.
[15]	AO	The PID controller's parameters were optimized for DC motor speed control using the AO technique. When compared to alternative techniques, AO offered superior control response, lowering error values and settling time.
[16]	AOA - DFO	PID settings were optimized using the AOA and DFO methods. Comparisons based on the ITAE criterion showed that DFO delivered lower overshoot and faster convergence, outperforming other methods.
[17]	OBL - HGSO	The HGSO algorithm was improved with opposition-based learning (OBL) to optimize PID controller parameters. The resulting OBL-HGSO algorithm achieved higher stability, shorter settling time, and stronger disturbance rejection compared to classical HGSO and other advanced algorithms.
[18]	POA	The POA technique was utilized to optimize a multi-stage FOPD(1+PI) controller. In comparison to PID and FOPID controllers, better control performance was attained with shorter rise and settling periods, reduced overshoot, and a smaller steady-state error.
[19]	ALO	PID controller gains were optimized using the ALO algorithm based on the ITAE criterion. Results showed that the ALO-PID structure provided faster and more stable responses compared to powerful algorithms such as HHO, GWO, SCA, and ASO.
[20]	GWO	The GWO algorithm was used to FOPID controller for DC motor speed control. Shorter rise and settling times, as well as increased stability, were the outcomes of optimization utilizing the ITAE performance index.
[21]	SFS (FOPID)	The FOPID controller parameters were optimized using the SFS technique. Optimization based on the ITAE criterion yielded high robustness against system parameter changes, lower error, and reduced settling time compared to other methods.
[22]	SFS (PI+DF)	A newly developed PI+DF controller structure is optimized using the SFS algorithm. Compared to PSO and classical methods, SFS provides lower overshoot, shorter settling time, and more stable speed response. The results were validated through both simulations and experimental tests on a DSP-based DC servo system.
[23]	SOS	PI controller parameters are optimized using the SOS algorithm. Compared with PSO, GA, and the Ziegler–Nichols method, SOS showed superior tracking performance and disturbance rejection. The proposed method was implemented in real time using a DSP-based control system.
[24]	SOS	This study, evaluated only in simulation, uses the SOS algorithm to optimize PI parameters. It outperformed GA by 2.1% in terms of maximum overshoot and by 25% in settling time; compared to Ziegler–Nichols, it achieved 73% better settling time. Robustness was also demonstrated with an average deviation of 18.2% under parameter variation.
[25]	FLC	An adaptive PI controller is proposed, in which Kp and Ki parameters are continuously updated using fuzzy logic. A PD-type FLC with two separate rule bases is used. According to simulations, this controller outperforms traditional PI controllers in terms of resilience to changes in load and transient responsiveness.
[26]	SSA	An exponential PI (EXP-PI) controller is proposed, where a nonlinear exponential gain block modifies the error before entering the PI controller. The controller parameters, including exponential slope and scale, are optimized using SSA. Real-time experiments confirmed superior speed tracking and torque disturbance rejection performance compared to fixed-gain PI controllers.

This work proposes the Artificial Hummingbird Algorithm (AHA) for the PID controller-based DC motor speed control problem. The AHA has been successfully applied to various engineering optimization problems, and it was selected in this study due to its strong balance between exploration and exploitation, which is critically important in tuning PID controllers for nonlinear and time-varying systems such as DC motors.

There are five major phases of this investigation. First, the suggested AHA algorithm is explained in full in Section 2. The study's materials and procedures, as well as the experimental setup and modelling procedure, are then described in Section 3. The collected data is examined and the results are tabulated in Section 4. The study's general conclusions are outlined in Section 5, along with how the findings support its inclusion in the literature.

2. ARTIFICIAL HUMMINGBIRD ALGORITHM

The AHA is a new meta-heuristic optimization method that is inspired by nature and imitates hummingbirds' nectar-foraging behaviours [27]. AHA is based on three different flight abilities: axial, diagonal, and omnidirectional. Combining these flight capabilities with other search strategies enhances the algorithm's search and extraction capabilities. Additionally, the system mimics a range of foraging behaviours, such as territorial, directed, and migration foraging.

- Initialization

  There are N potential solutions (hummingbirds) in the population at the start of the procedure. These individuals are randomly generated within the defined solution space;

  $$Xj = LB + r \times (UB - LB), j = 1,2,\ldots,N \quad (1)$$

  In this case, Xj stands for the location of the j-th hummingbird, or the potential solution. The LB and UB symbols define the minimum and maximum thresholds within the search space, respectively. $r \in [0,1]$ is a random no. that is evenly dispersed within the interval [0,1]. Additionally, the algorithm stores the best solutions previously visited by each individual in a visit table. The meaning of this table is as listed below;

  $$VT_{j,i} = \begin{cases} 0, & if \quad j \neq i \\ null & j = i \end{cases}, j = 1,,,N, i = 1,.,N \quad (2)$$

  Here, $VT_{j,i}$=0 indicates that the j-th hummingbird has visited the i-th food source, while $VT_{j,i} = null$ represents the hummingbird's own consumption amount.

- Guided Foraging

  At this point, the hummingbird uses the food source from the visit table with the highest nectar renewal rate—that is, the best solution—as a pointer to choose a new one. This strategy is applied according to three different types of flights:

  Axial Flight:

  $$D^i = \begin{cases} 1, & if \quad i = R \\ 0, & else \end{cases}, \; i = 1,\ldots,d, \quad (3)$$

  Diagonal Flight:

  $$D^i = \begin{cases} 1, & if\ i = P(j) \\ 0, & else \end{cases}, \; j \in [1,k], \; i = 1,\ldots,d, \quad (4)$$

  Here $P = randperm(k), k \in [2,[r1(d-2),]+1]$.

  Omnidirectional Flight:

  $$D^i = 1 \quad i = 1,\ldots,d \quad (5)$$

  The following is a model of the guided foraging flight;

  $$V_i(t+1) = X_{i,t}(t) + a \times D \times (X_i(t) - X_{i,t}(t)), \quad a \in N(0,1) \quad (6)$$

  The rule that follows is used to update the new solution;

  $$X_i(t+1) = \begin{cases} V_i(t+1), if\ f(Vi(t+1)) \leq f(Xi(t)) \\ X_i, \qquad\qquad else \end{cases} \quad (7)$$

  Here, $f(\cdot)$ denotes the fitness function.

- Territorial Foraging

  After consuming a nectar source, the hummingbird tends to search for a new source in a nearby area. In this case, a slightly different position is selected from the current solution with a small step;

  $$V_i(t+1) = X_{i,t}(t) + b \times D \times (X_i(t) - X_{i,t}(t)), \quad b \in N(0,1) \quad (8)$$

  This approach mimics local search behaviour.

- Migration Foraging

  When the food source where the hummingbird is located becomes insufficient, it migrates to a new random area. The solution with the lowest fitness value exhibits this behaviour. The following is the definition of the new role;

  $$X_w(t+1) = LB + r \times (UB - LB) \quad (9)$$

  The person with the lowest fitness value is denoted by X_w in this case. The major steps of the AHA algorithm and the flow based on the foraging behaviour of hummingbirds are summarized in Figure 1.

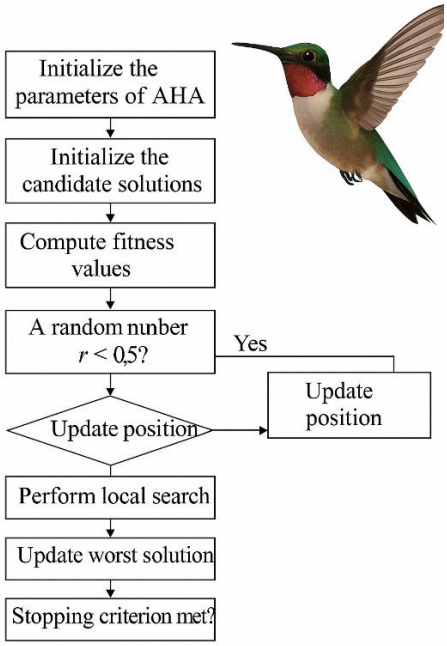

Figure 1. Flowchart of the AHA.

3. MATERIALS AND METHODS

3.1. DC Motor Model

In this study, a DC motor that was externally triggered was used. Figure 2 presents the circuit configuration of a DC motor under armature control. The motor parameters used in this study are adapted from reference models commonly used in the literature for permanent magnet DC motors. These values fall within realistic ranges and are representative of small-scale motors found in industrial and educational environments.

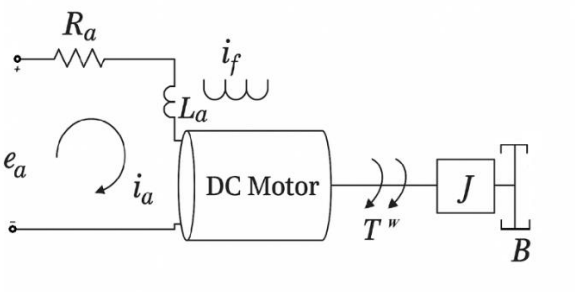

Figure 2. The equivalent diagram of a DC motor controlled via its armature.[28]

In this configuration, the motor's rotational speed (ωs controlled by the armature voltage, represented by e_a. In this study, e_a denotes the externally applied armature voltage, which acts as the system input. It should not be confused with the machine's internal back electromotive force (e_b), which is separately defined and denoted accordingly. The rotating rotor interacts with a constant magnetic field. Therefore, the voltage induced at the terminals, known as the back electromotive force (EMF) (e_b), is directly proportional to the speed (ω=dΘ/dt).

$$e_b = K_b \frac{d\theta}{dt} \quad (10)$$

Where the back EMF constant is denoted by K_b. Equation (11) provides the armature circuit mathematical representation.

$$e_a = \mathrm{L}\frac{di_a}{dt} + Ri_a + e_b \quad (11)$$

Where L is the armature winding's inductance, R the armature resistance and i_a is the armature current. The armature current (i_a) and the torque (T_m) produced by the motor are proportional.

$$T_m = K_t i_a \quad (12)$$

Where the motor torque constant is K_t. Considering the friction coefficient (f) and the moment of inertia (J), the torque equation is given as;

$$T_m = J\frac{d^2\theta}{dt^2} + f\frac{d\theta}{dt} \quad (13)$$

After applying Laplace transforms to Equations (10), (11), and (13) and assuming zero initial conditions, Equation (14) provides the speed-controlled DC motor's resulting transfer function [29];

$$G_m(s) = \frac{w(s)}{e_{a(s)}} = \frac{K_t}{(L_s+R)(J_S+f)+K_bK_t} \quad (14)$$

Table 2 lists the DC motor's parameter values used in this investigation.

Table 2. DC motor specifications.

Parameter	Value
R	0.4 Ω
L	2.7 H
J	0.0004 kg.m^2
B	0.0022 N·m·s/rad
K	0.015 N·m/A
Kb	0.05 V·s

3.2. PID Controller Architecture for DC Motor Speed Control

To enhance the DC motor speed control's performance, a PID controller was employed. Equation (15) provides the closed-loop function of transfer for the DC motor using the PID controller as shown in Figure 3 [30].

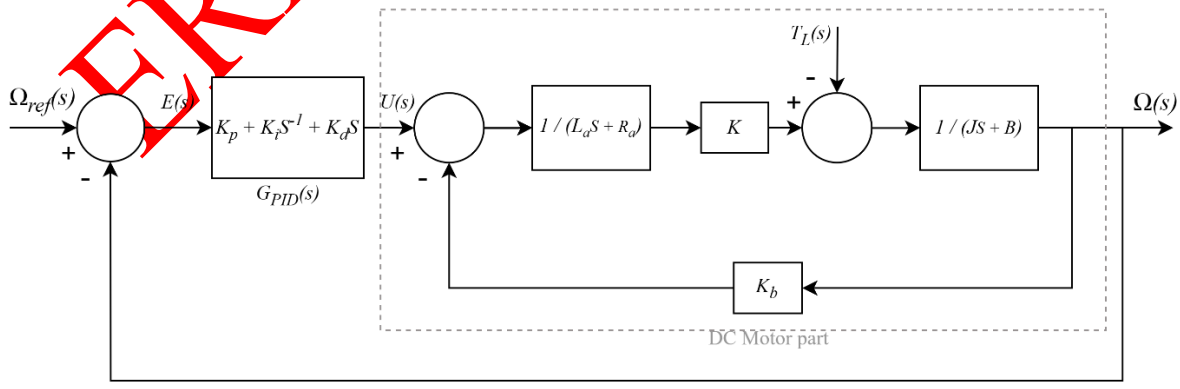

Figure 3. Block schematic of a PID-controlled DC motor system.

$$G_{PID-Motor}(s) = \begin{cases} \frac{\Omega(s)}{\Omega_{ref}(s)} = \frac{0.015(k_d s^2+k_p s+k_i)}{0.00108s^3+0.0061s^2+0.00163s+0.015(k_d s^2+k_p s+k_i)}, & T_L = 0 \\ \frac{\Omega(s)}{\Omega_{ref}(s)} = \frac{(2.7s+0.4)s}{0.00108s^3+0.0061s^2+0.00163s+0.015(k_d s^2+k_p s+k_i)}, & E_a = 0 \end{cases}$$

[31](15)

To analyse the system's inherent dynamics without the influence of a controller, the open-loop transfer function between the applied armature voltage E_a and the angular speed $\Omega(s)$ is considered. In the case where $E_a = 0$, no input is applied to the system, and hence $\Omega(s)/\Omega_{ref}(s)$ is not meaningful. Instead, the system's response can be evaluated using the transfer function $\Omega(s)/T_L(s)$, where $T_L(s)$ denotes the external load torque. This approach is useful in terms of the natural solution of the system without the controller effect.

4. ANALYSES AND FINDINGS

The proposed AHA was simulated in the MATLAB 2024a environment. In this study, conducted for the optimization of DC motor speed control, four different error criteria were used to evaluate the system's performance more fairly and comprehensively: ITAE, IAE, ISE, ITSE. The error functions are given in Equations (16)– (19).

$$\text{ITAE} = \int_0^\infty t|e(t)|dt \quad (16)$$

$$\text{ITSE} = \int_0^\infty t\,e^2(t)dt \quad (17)$$

$$ISE = \int_0^\infty e^2(t)dt \quad (18)$$

$$IAE = \int_0^\infty |e(t)|dt \quad (19)$$

To assess how well the suggested algorithm works, comparisons were made with HHO [32], ASO [33], GWO [20], SCA [34], IWO [35], and SFS [21], which are frequently used in the literature and have achieved successful results. This comparison is presented in Table 4. During the optimization process, the maximum number of iterations was set to 30 and the number of search agents to 50. The lower limits for the controller gains were set to 0.001 for K_p, K_i and K_d, while the upper limits were assigned as 20 for each gain. Table 3 displays the AHA-PID controller's control gains, which were optimized based on the ITAE objective function, as well as those of the other controllers.

The comparison findings are shown in Table 3 for the three primary metrics—percentage overshoot (M_p), settling time (t_s), and rising time (t_r)—that are used to assess the transient response performance of control systems. In this table, the best results obtained during the simulation process are highlighted in bold. The graphic shows that the AHA-based PID controller has the shortest rise and settling times for DC motor speed control. This enables the system to reach the target value more quickly and stably. The reactions of several controllers to a unit step input supplied to the DC motor system are graphically compared in Figure 4. Evaluations based on this figure reveal that the AHA-PID controller offers a faster and more stable response in terms of dynamic performance compared to other control methods. In particular, its rapid initial rise and quick stabilization indicate an improvement in the transient regime performance. These findings show that the AHA algorithm provides notable benefits for improving system response and is a useful tool for optimizing PID parameters. The following definitions apply to the transitory performance criteria employed in this study: The amount of time needed for the system output to enter and stay inside the ±2% tolerance band surrounding the reference value is known as the "settling time." The rise

Table 3. PID gains and transient characteristic values.

Alg.	K_p	K_i	K_d	M_p	t_s	t_r
AHA-PID	18.782	5.0201	3.325	**0.0000**	**0.08470**	**0.04757**
HHO-PID	15.858	3.696	2.773	**0.0000**	0.10032	0.05680
ASO-PID	11.944	2.052	2.436	**0.0000**	0.15347	0.06916
GWO-PID	6.898	0.563	0.929	1.5093	0.20522	0.13881
SCA-PID	4.501	0.526	0.53	2.3093	0.49031	0.20378
IWO-PID	1.5782	0.4372	0.0481	6.9759	1.2533	0.41887
SFS-PID	1.6315	0.2798	0.2395	**0.0000**	1.4475	0.54362

Table 4. Comparison of PID controller performances based on error criteria.

Alg.	ITAE	IAE	ISE	ITSE
AHA-PID	**0.000470**	**0.02167**	**0.01085**	**0.000116**
HHO-PID	0.001967	0.02696	0.01300	0.000168
ASO-PID	0.007478	0.03916	0.05117	0.000261
GWO-PID	0.022313	0.08175	0.03626	0.001363
SCA-PID	0.030701	0.12081	0.05843	0.003197
IWO-PID	0.085293	0.31385	0.19271	0.026661
SFS-PID	0.089975	0.27715	0.12603	0.017824

time is the length of time needed for the resultant value to rise from 10% to 90% of the constant state value. The overestimation rate is the percentage that separates the maximum value of the system output and the steady-state value.

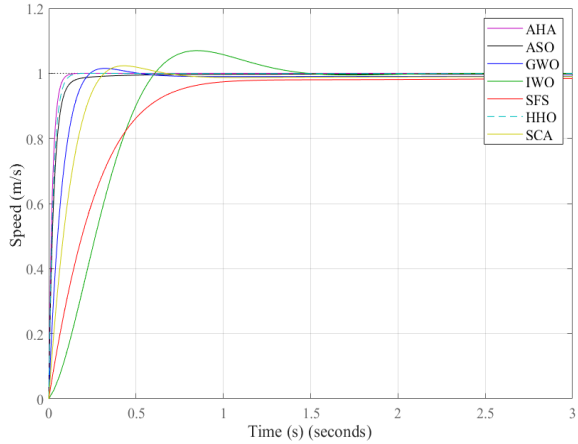

Figure 4. Step responses of the PID controllers.

Figure 5 displays the Convergence Curve of Algorithms in PID Optimization. The curve represents the best ITAE fitness value obtained during each of the 30 iterations. As seen in the plot, the algorithm exhibits a rapid reduction in error within the first few iterations and converges to a stable minimum value around the 15th iteration, demonstrating effective search and stability.

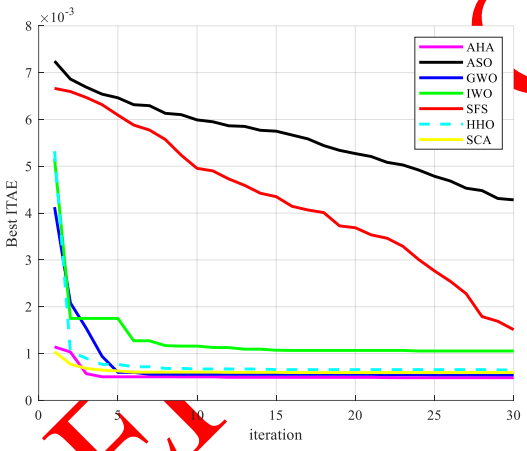

Figure 5. Convergence Curve of Algorithms in PID Optimization

4.1. Robustness Analysis Against Different Parameters

The robustness of the suggested AHA-based PID controller against changes in DC motor parameters was thoroughly examined and contrasted with PID controllers derived from various optimization techniques in this study. Within the scope of the study, four different operating scenarios were created by varying the motor's armature resistance (R_a) ±50% and the motor torque constant (K) ±40%, as shown in Table 6.The unit step responses obtained under these operating conditions are presented comparatively in Figures 6–9, and the transient characteristics are detailed in Tables 6–9.The analyses revealed that the AHA-based PID controller exhibited

Table 5. Four different operating scenarios for the DC motor.

İnstance	R_a	K
I.	0.20	0.009
II.	0.20	0.021
III.	0.60	0.009
IV.	0.60	0.021

lower rise times, shorter settling times, and, in many cases, lower maximum overshoot values compared to controllers designed with other methods, despite the parameter variations. These outcomes unequivocally show that, even when system parameters change, the AHA-based PID controller offers a high degree of robustness and dependability.

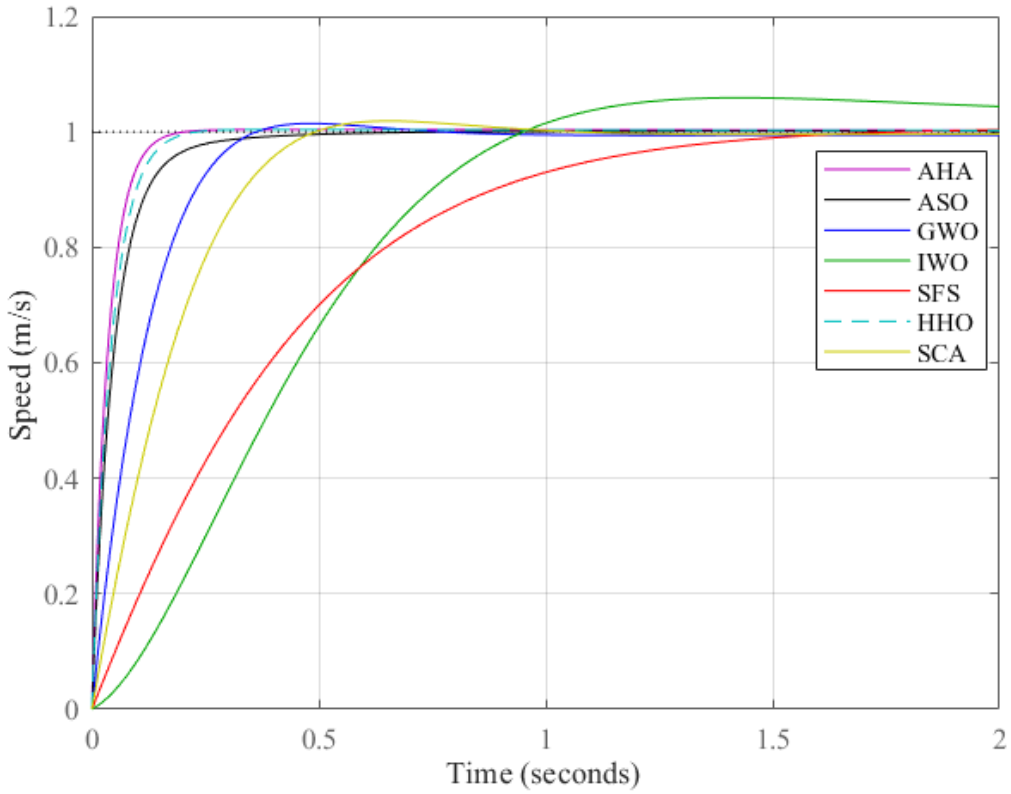

Figure 6. DC motor step responsiveness of controllers with Ra = 0.20 and K = 0.009.

Table 6. Comparison of the controllers' error numbers and transient response outcomes in instance I.

Alg.	M_p	t_s	t_r	ITAE	IAE	ISE	ITSE
AHA-PID	0.3068	**0.1362**	**0.0785**	0.0077	**0.0416**	**0.0180**	**0.0003**
HHO-PID	0.3758	0.1601	0.0934	0.0074	0.0477	0.0215	0.0004
ASO-PID	**0.0000**	0.2547	0.1176	**0.0056**	0.0564	0.0254	0.0006
GWO-PID	1.4454	0.3153	0.2157	0.0200	0.1138	0.0581	0.0030
SCA-PID	1.8829	0.4403	0.3107	0.0292	0.1668	0.0917	0.0072
IWO-PID	5.9002	4.1872	0.6356	0.1861	0.4571	0.2761	0.0561
SFS-PID	0.6305	1.3557	0.8340	0.1384	0.3981	0.2154	0.0423

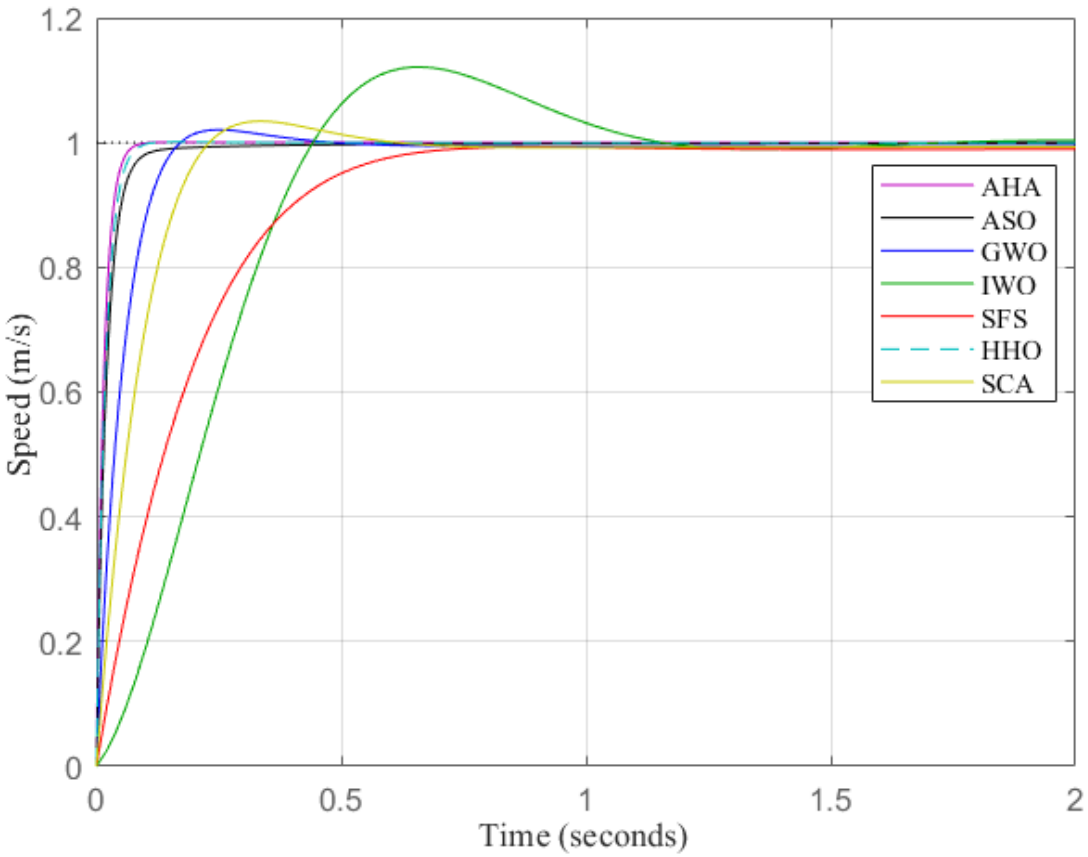

Figure 7. DC motor step responsiveness of controllers R_a =0.20 and K=0.021.

Table 7. Comparison of the controllers' error numbers and transient response outcomes in instance II.

Alg.	**M_p**	**t_s**	**t_r**	**ITAE**	**IAE**	**ISE**	**ITSE**
AHA-PID	0.0196	**0.0598**	**0.0339**	**0.0007**	**0.0160**	**0.0075**	**0.0001**
HHO-PID	0.0803	0.0709	0.0405	0.0007	0.0188	0.0093	0.0001
ASO-PID	**0.0000**	0.0982	0.0483	0.0042	0.0269	0.0107	0.0001
GWO-PID	2.0544	0.2677	0.1018	0.0143	0.0601	0.0262	0.0007
SCA-PID	3.4288	0.4555	0.1513	0.0201	0.0915	0.0429	0.0017
IWO-PID	12.1200	1.0453	0.3148	0.0716	0.2687	0.1545	0.0188
SFS-PID	0.0803	0.6247	0.3781	0.0461	0.1929	0.0975	0.0089

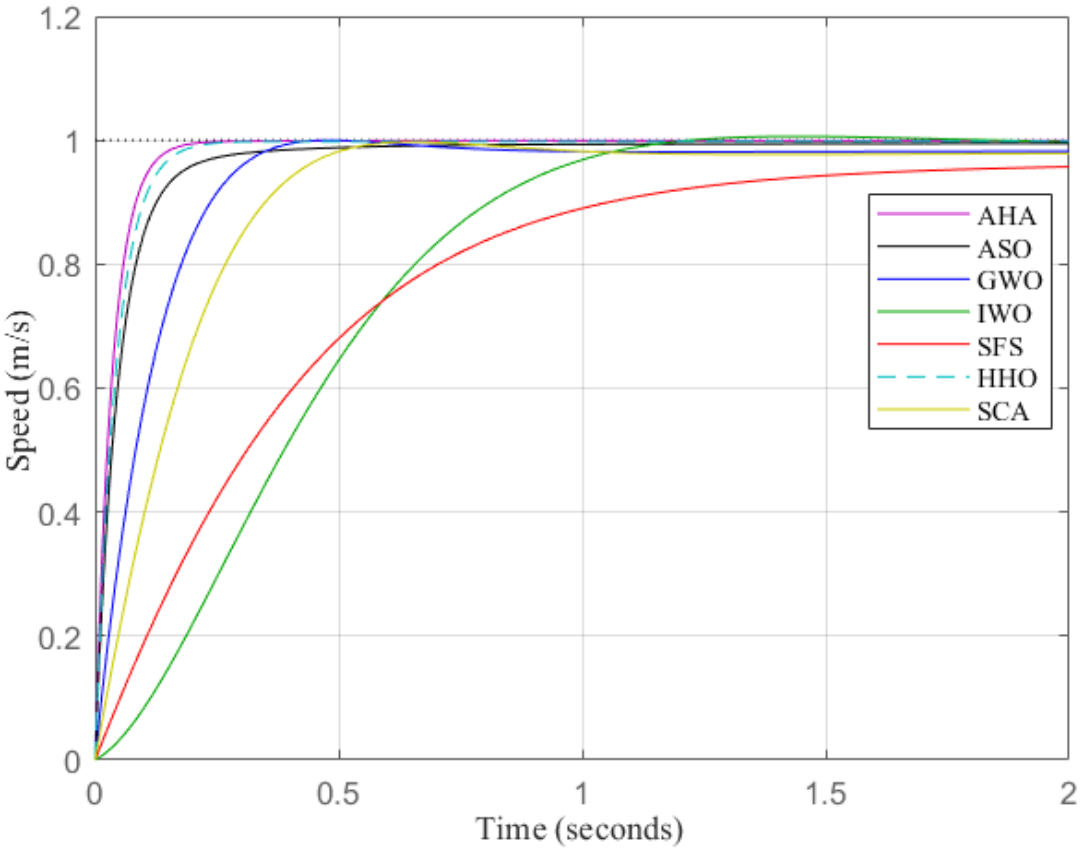

Figure 8. DC motor step responsiveness of controllers R_a =0.60 and K=0.009.

Table 8. Comparison of the controllers' error numbers and transient response outcomes in instance III.

Alg.	**M_p**	**t_s**	**t_r**	**ITAE**	**IAE**	**ISE**	**ITSE**
AHA-PID	**0.0000**	**0.1446**	**0.0799**	**0.0025**	**0.0376**	**0.0181**	**0.0002**
HHO-PID	**0.0000**	0.1714	0.0953	0.0055	0.0467	0.0217	0.0005
ASO-PID	**0.0000**	0.3177	0.1209	0.0159	0.0676	0.0257	0.0008
GWO-PID	**0.0000**	0.3436	0.2236	0.0417	0.1309	0.0592	0.0037
SCA-PID	2.5747	2.5747	0.3261	0.0577	0.1888	0.0936	0.0082
IWO-PID	0.6250	1.0551	0.6968	0.1309	0.4317	0.2805	0.0560
SFS-PID	6.1575	6.1575	1.0030	0.2190	0.4622	0.2278	0.0523

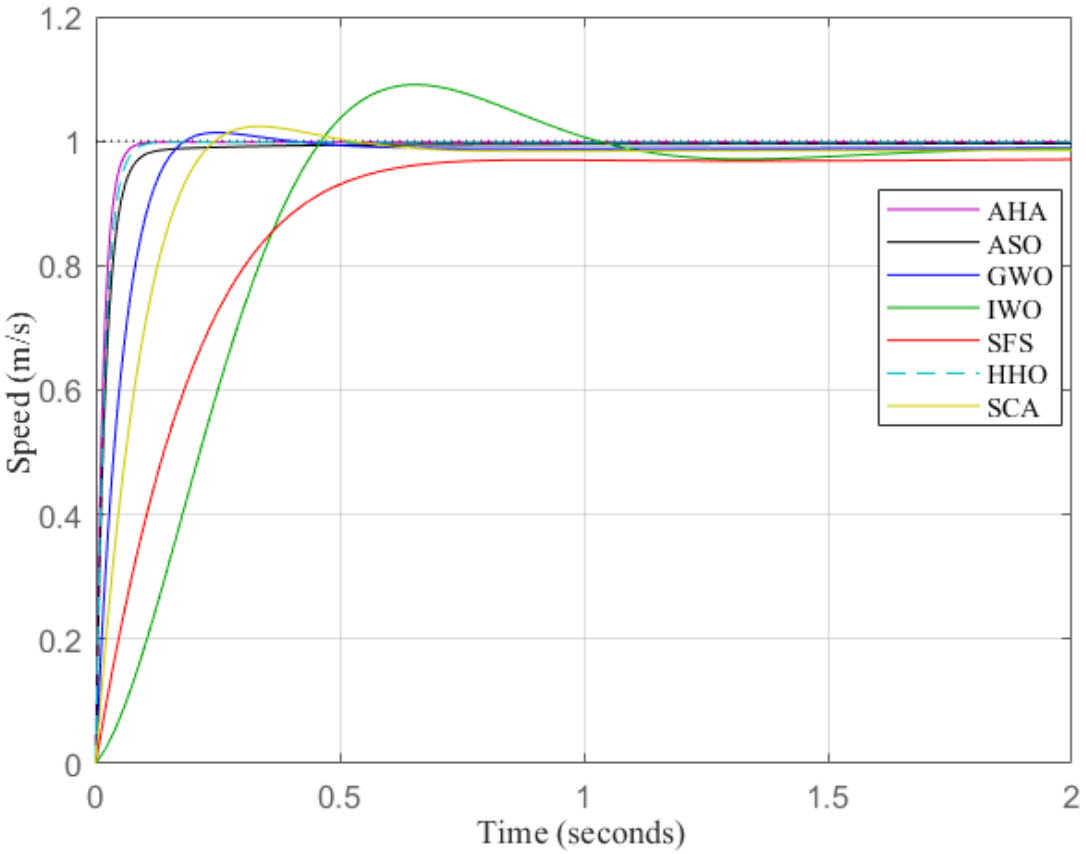

Figure 9. DC motor step responsiveness of controllers R_a =0.60 and K=0.021.

Table 9. Comparison of the controllers' error numbers and transient response outcomes in instance IV.

Alg.	M_p	t_s	t_r	ITAE	IAE	ISE	ITSE
AHA-PID	**0.0000**	**0.0614**	**0.0341**	**0.0030**	**0.0184**	**0.0078**	**0.0001**
HHO-PID	**0.0000**	0.0731	0.0408	0.0047	0.0228	0.0093	0.0001
ASO-PID	**0.0000**	0.1058	0.0489	0.0100	0.0328	0.0108	0.0002
GWO-PID	1.3700	0.1558	0.1036	0.0242	0.0675	0.0265	0.0009
SCA-PID	2.3703	0.3869	0.1548	0.0335	0.1008	0.0434	0.0021
IWO-PID	9.0808	1.6260	0.3250	0.0814	0.2697	0.1542	0.0178
SFS-PID	**0.0000**	4.2741	0.4071	0.0868	0.2297	0.1008	0.0111

4.2. Variable Speed Analysis

This study segment looked at how the developed PID controllers responded to a reference speed signal that changed over time [36]. To better represent speed changes that may occur in real-world systems, the reference signal was gradually modified at specific time intervals. Initially, between 0–5 seconds, the system operated at a speed of 1 rad/s. Then, between 5–10 seconds, the speed was doubled. Following this increase, the system speed was reduced back to 1 rad/s between 10–15 seconds. Between 20–25 seconds, the system's angular speed was lowered to one-fourth (0.25 rad/s) to simulate a weak operating condition. Finally, between 25–30 seconds, the speed was returned to its nominal value of 1 rad/s. Each PID controller's transient and steady-state performances were compared using this reference profile. The results observed in Figures 10–11 demonstrate the controllers' ability to adapt to dynamic load variations. Particularly, the adaptability of the AHA-based PID controller under these varying conditions indicates its superior performance in maintaining system stability and achieving fast response times.

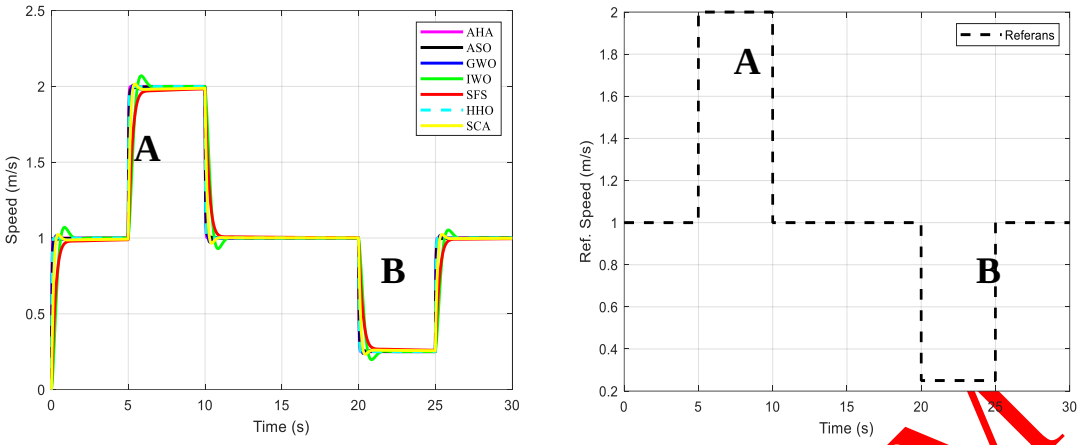

Figure 10. Time-varying reference speed signal and PID controller responses.

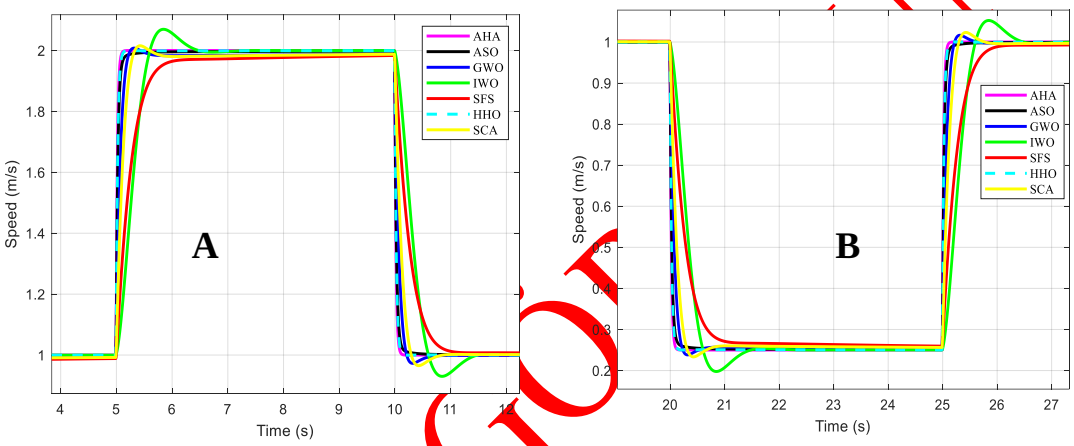

Figure 11. PID controller responses during sudden changes in the reference speed: (A) Sudden speed drop, (B) Sudden speed increase.

4.3. Disturbance Rejection Capability Analysis

The system was tested under various load scenarios to assess the suggested controller's resilience and disturbance rejection capabilities. First, the system was subjected to time-varying load effects and the speed tracking performance of the control algorithms was examined. As seen in Figure 12a, the proposed algorithm reached the reference speed quickly despite the load changes and showed minimum overshoot. Then, positive sudden load disturbances were applied at 1.5 seconds and negative sudden load disturbances at 2.2 seconds. Figure 12b shows that the proposed controller provides fast recovery with minimum deviation against these disturbances. It was observed that other algorithms either recovered more slowly or produced larger permanent errors. These findings reveal that the proposed method exhibits stable and reliable performance under different load effects.

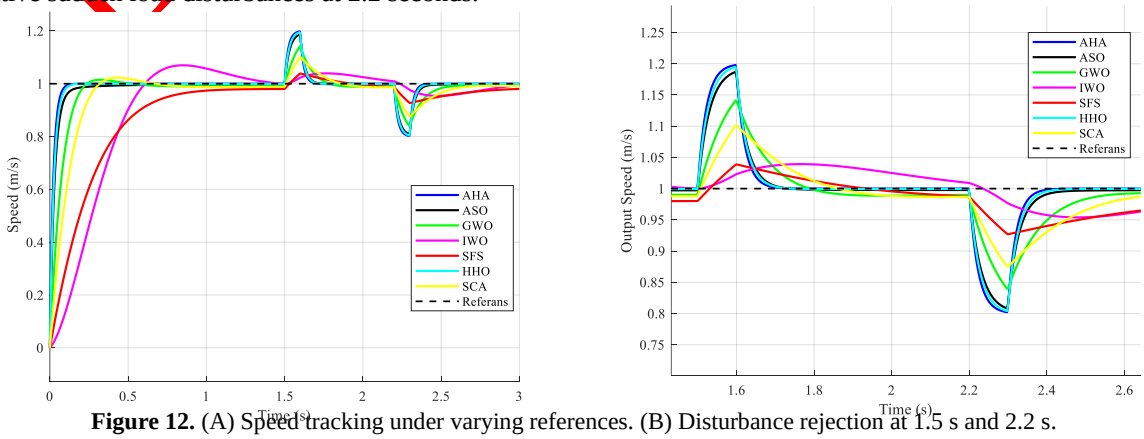

Figure 12. (A) Speed tracking under varying references. (B) Disturbance rejection at 1.5 s and 2.2 s.

5. CONCLUSION

For the DC motor speed control problem, this research proposed a PID controller that was optimized using the AHA. Thanks to the AHA's nature-inspired guided, territorial, and migratory foraging strategies, the PID gains were effectively and rapidly optimized. Within the scope of the simulations carried out, the AHA-PID controller was compared with PID controllers obtained using widely adopted algorithms in the literature, such as HHO, ASO, GWO, SCA, IWO, and SFS. The results indicated that the AHA-PID structure outclassed the others, especially regarding transient response characteristics. Attaining the minimum values in key metrics such as the rise time and the settling time enabled the system to reach the reference value quickly and stably. Moreover, the system's robustness against parameter variations (e.g., armature resistance and torque constant) was comprehensively analysed. Analyses conducted under different operating scenarios revealed that the AHA-PID controller exhibited a high degree of robustness and was relatively less affected by system parameter variations. This finding supports its potential to provide a reliable and flexible control solution in industrial applications. Finally, in tests conducted under time-varying reference signals, the AHA-PID controller demonstrated the fastest adaptation to sudden speed changes, achieving superior reference tracking performance. Overall, AHA offers a high-performance solution for managing intricate dynamic systems, like DC motor speed management, and is a useful technique for adjusting PID controller parameters, according to all of these findings.

DECLARATION OF ETHICAL STANDARDS

The authors of this article declare that ethical committee approval and/or legal/special permission were not required for the materials and methods used in their study.

AUTHORS CONTRIBITIONS

Kadir Yasin SUNCA: Finished writing the article after doing the simulation studies and analysing the findings.
Ali Fuat BOZ: Finished writing the article after evaluating the findings.

CONFLICT OF INTEREST

The authors declare no conflict of interest.

REFERENCES

[1] A. F. Güven, "Exploring Solar Energy Systems: A Comparative Study of Optimization Algorithms, MPPTs, and Controllers," ***IET Control Theory& Applications*** (18)7:887–920., (2024).

[2] Ekinci S. and Hekimoğlu B., "Improved kidney-inspired algorithm approach for tuning of PID Controller in AVR system". ***IEEE Access*** 7: 39935–39947. (2019).

[3] Xia, C. L., "Permanent magnet brushless DC motor drives and controls." ***John Wiley & Sons***. (2012).

[4] Gamazo-Real, J. C., Vázquez-Sánchez, E., & Gómez-Gil, J. "Position and speed control of brushless DC motors using sensorless techniques and application trends". ***Sensors***, 10(7), 6901-6947. (2010).

[5] Zhao, X., Sun, Y., Li, Y., Jia, N., & Xu, J. "Applications of machine learning in real-time control systems: a review."***Measurement Science and Technology***., (2024).

[6] Saini R., Parmar G., Gupta R. SFS based Fractional Order "PID Controller (FOPID) for Speed Control of DC Motor." ***International Journal***, 9 (4)., (2020).

[7] Wang M.S., Chen S.C., Shih C.H. "Speed control of brushless DC motor by adaptive network-based fuzzy inference." ***Microsystem Technologies***, 24 (1): 33-39. (2018).

[8] Varshney A., Gupta D., Dwivedi B. "Speed response of brushless DC motor using fuzzy PID controller under varying load condition." ***Journal of Electrical Systems and Information Technology***, 4 (2): 310-321. (2017).

[9] Dursun E.H., Durdu A. "Speed control of a DC motor with variable load using sliding mode control." ***International Journal of Computer and Electrical Engineering***, 8 (3): 219-226. (2016).

[10] Jacquot RG., "Modern digital control systems", ***Routledge***. (2019).

[11] Design and application of an optimally tuned PID controller for DC motor speed regulation via a novel hybrid Le´vy flight distribution and Nelder–Mead algorithm

[12] Güven, A. F., Mengi, O. Ö., Elseify, M. A., & Kamel, S. "Comprehensive optimization of PID controller parameters for DC motor speed management using a modified jellyfish search algorithm." ***Optimal Control Applications and Methods***, 46(1), 320-342., (2025).

[13] Alkrwy, A., Hussein, A. A., Atyia, T. H., & Khamees, M. "Adaptive tuning of PID controller using crow Search algorithm for DC motor." ***In IOP Conference Series***: ***Materials Science and Engineering*** (Vol. 1076, No. 1, p. 012001). IOP Publishing., (2021).

[14] Idir, A., Khettab, K., & Bensafia, Y., "Design of an optimally tuned fractionalized PID controller for dc motor speed control via a henry gas solubility optimization algorithm." ***Int. J. Intell. Eng. Syst***, 15(2), 59. (2022).

[15] Aribowo, W., Supari, S., & Suprianto, B. "Optimization of PID parameters for controlling DC motor based on the aquila optimizer algorithm." ***International Journal of Power Electronics and Drive Systems***, 13(1), 216., (2022).

[16] Acharya, B. B., Dhakal, S., Bhattarai, A., & Bhattarai, N. "PID speed control of DC motor using meta-heuristic algorithms." ***International Journal of Power Electronics and Drive Systems***, 12(2), 822., (2021).

[17] Ekinci, S., Hekimoğlu, B., & Izci, D., "Opposition based Henry gas solubility optimization as a novel algorithm for PID control of DC motor." ***Engineering Science and Technology, an International Journal***, 24(2), 331-342. (2021).

[18] Jabari, M., Ekinci, S., Izci, D., Bajaj, M., & Zaitsev, I. "Efficient DC motor speed control using a novel multi-stage FOPD (1+ PI) controller optimized by the Pelican

optimization algorithm." ***Scientific Reports***, 14(1), 22442. (2024).

[19] Musa, M. A., & Jayachitra, T., "Ant Lion Optimization Based PID Controller in DC Motor Speed Control." In 2024 ***International Conference on Electrical Electronics and Computing Technologies (ICEECT)*** (1):1-6. IEEE., (2024).

[20] Agarwal, J., Parmar, G., Gupta, R., & Sikander, A. "Analysis of grey wolf optimizer based fractional order PID controller in speed control of DC motor." ***Microsystem Technologies***, 24, 4997-5006. (2018).

[21] Khanam I., Parmar G. "Application of SFS algorithm in control of DC motor and comparative analysis." In 2017 ***4th IEEE Uttar Pradesh Section International Conference on Electrical, Computer and Electronics (UPCON)***, October, 256-261., (2017).

[22] Çelik, E., & Gör, H., "Enhanced speed control of a DC servo system using PI+ DF controller tuned by stochastic fractal search technique. Journal of the Franklin Institute, 356(3), 1333-1359., (2019).

[23] Celik, E., & Öztürk, N., "First application of symbiotic organisms search algorithm to off-line optimization of PI parameters for DSP-based DC motor drives." ***Neural Computing and Applications***, 30, 1689-1699. (2018).

[24] Çelik, E., & Öztürk, N., "Doğru akım motor sürücüleri için PI parametrelerinin simbiyotik organizmalar arama algoritması ile optimal ayarı." ***Bilişim Teknolojileri Dergisi***, 10(3), 311-318., (2017).

[25] Çelik, E., Dalcali, A., Öztürk, N., & Canbaz, R., "An adaptive PI controller schema based on fuzzy logic controller for speed control of permanent magnet synchronous motors." In ***4th international conference on power engineering, energy and electrical drives (pp. 715-720). IEEE***. (2013).

[26] Çelik, E., Bal, G., Öztürk, N., Bekiroglu, E., Houssein, E. H., Ocak, C., & Sharma, G., "Improving speed control characteristics of PMDC motor drives using nonlinear PI control." ***Neural Computing and Applications***, 36(16), 9113-9124., (2024).

[27] Zhao, W., Wang, L., & Mirjalili, S., "Artificial hummingbird algorithm: A new bio-inspired optimizer with its engineering applications." ***Computer Methods in Applied Mechanics and Engineering***, 388, 114194., (2022).

[28] Başlık Ş., Sesli E. and Akyazı Ö., "Effect of derivative filter usage on a pıd controller optimized via pathfinder algorithm: an example of a DC-MSCS", ***Journal of Polytechnic***, 27(1): 185-196, (2024).

[29] Hekimoğlu, B., "Böbrek-ilhamlı algoritma ile ayarlanan PID kontrolör kullanarak DC motor hız kontrolü." ***Bitlis Eren Üniversitesi Fen Bilimleri Dergisi***, 8(2), 652-663. (2019).

[30] Şahin, A. K., Akyazı, Ö., Sahın, E., & Çakır, O., "DC Motorun hız kontrolü için meta-sezgisel algoritma tabanlı PID denetleyici tasarımı". ***Bitlis Eren Üniversitesi Fen Bilimleri Dergisi***, 10(2), 533-549. (2021).

[31] Çavdar B., Şahin E. ve Nuroğlu F.M., "Doğru akım motoru hız kontrolü için SAA tabanlı kesir dereceli PI-PD eklemeli denetleyici tasarımı", ***Journal of Polytechnic***, 27(1): 283-296, (2024).

[32] S. Ekinci, D. Izci, and B. Hekimoglu, "PID Speed Control of DC Motor Using Harris Hawks Optimization Algorithm," in 2020 ***International Conference on Electrical, Communication, and Computer Engineering (ICECCE)***, IEEE, Jun. 1–6. (2020).

[33] B. Hekimoglu, "Optimal Tuning of Fractional Order PID Controller for DC Motor Speed Control via Chaotic Atom Search Optimization Algorithm," ***IEEE Access***, (7):38100–38114, (2019).

[34] J. Agarwal, G. Parmar, and R. Gupta, "Application of sine cosine algorithm in optimal control of DC motor and robustness analysis," ***Wulfenia J***, 24(11):77–95, (2017).

[35] Khalilpour R., Razmjooy A., Hosseini H., Moallem P. "Optimal control of DC motor using invasive weed optimization.", (2011).

[36] Sonugür G., "DA motor kontrolünde veri güdümlü ve model tabanlı yöntemlerin ani yük değişimlerine karşı tepkilerinin analizi", ***Journal of Polytechnic***, 27(5): 1721-1732, (2024).